Article

Building up and Characterization of Calcined Marl-Based Geopolymeric Cement

Galal El-Habaak [1], Mohamed Askalany [2] and Mahmoud Abdel-Hakeem [2,*]

[1]   Department of Geology, Faculty of Science, Assiut University, Assiut 71511, Egypt; habaak@yahoo.com
[2]   Department of Geology, Faculty of Science, South Valley University, Qena 83511, Egypt;
    mohamed.ibrahim11@sci.svu.edu.eg
*   Correspondence: mahmoud.sabry@sci.svu.edu.eg; Tel.: +20-960-1555-005 (ext. 219)

check for updates

Abstract: The present study mainly investigates the synthesis of calcined marl-based geopolymeric cement under different synthesis conditions including NaOH concentration, sodium silicate (SS)/sodium hydroxide (SH) mass ratios, solid (S)/liquid (L) mass ratios, calcination temperatures, curing temperatures, curing times, and aging intervals. The studied head sample was obtained from the Abu-Tartur phosphate mine in the Western Desert of Egypt and subjected to chemical and mineralogical characterizations using X-ray fluorescence (XRF), X-ray diffraction (XRD), and Fourier transform–infrared spectroscopy (FT–IR). Regarding calcination, this was conducted at 550, 650, 750, and 850 °C for one hour and resulted in thermal decomposition of calcite and saponite and the formation of new mineral phases including anthophyllite, wollastonite, and silica. On the other hand, the geopolymerization process was initiated by mixing the calcined marl sample with the alkali activation solution at different mixing ratios and varying curing conditions. The compressive strength measurements indicate that 750 °C, 12 M NaOH, 0.6 SS/SH mass ratio, 2 S/L mass ratio, 80 °C curing temperature, 12 h curing time, and 28 days aging time are considered all to be the optimum synthesis conditions of the Abu-Tartur calcined marl-based geopolymer.

Keywords: geopolymer; calcined marl; alkali activation; compressive strength

1. Introduction

Geopolymers are a subclass of alkali-activated materials. In order to obtain a geopolymer, aluminosilicates should have a $SiO_2 + Al_2O_3$ content >80 wt % and low CaO content. This reaction occurs at a wide range of temperatures varying between 20 and 90 °C and curing time between 6 and 48 h [1–3]. The mechanism of geopolymerization is explained through three main processes: (a) the dissolution of aluminosilicate material to form reactive silica and alumina ions; (b) the rearrangement of these ions into fundamental units called oligomers; and (c) a polycondensation process under exothermic conditions to create a network of three-dimensional amorphous to semi-crystalline microstructure. The latter consists of silica and alumina tetrahedrals linked to each other by sharing all the oxygen atoms, with the presence of positive ions (e.g., Na^+, K^+, Ca^{++}, etc.) to balance the negative charge of aluminum in geopolymer structure [4,5]. Recently, the polycondensation process has been studied using static nuclear magnetic resonance, which showed that during the polycondensation process two types of aluminosilicate gels are formed. The first one is a heterogeneous interstitial phase consisting of Al-rich gel and incorporated positive ions (e.g., Na^+) to compensate the negative charge of Al in the tetrahedral sites. This phase precipitates at the beginning of polycondensation, and then evolves into a denser gel consisting of polycondensed aluminate and silicate oligomers during a massive precipitation of all aluminosilicate species [6].
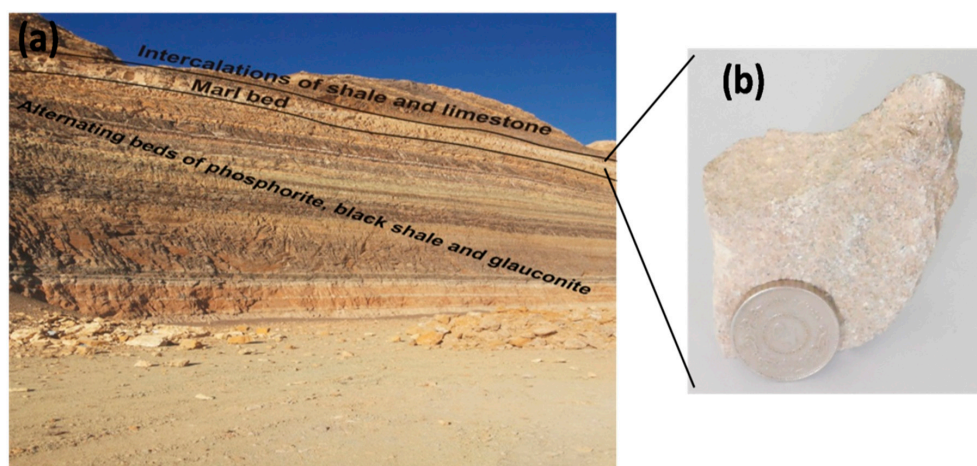
Geopolymers are novel and promising materials that compete in different industrial applications such as thermal insulation, immobilization of toxic wastes and concrete production [7,8]. Among all of these applications, the exploitation of geopolymers as partly and completely alternative materials to Portland cement is considered to be the most attractive trend for the development of a green construction industry. The Portland cement industry is one of the most energy-intensive industries due to the high temperatures (1250–1500 °C) required for converting the raw materials into cement clinker [9]. The rate of energy consumption during the manufacture of Portland cement is theoretically calculated 1.76 megajoule to yield 1 kg Portland clinker [10]. Moreover, the Portland cement industry is implicated in the increase of greenhouse gas emissions stemming from the burning of fossil fuel during the clinker production. The global production of about 2 billion tons of cement clinker emits about 6% CO_2 into the Earth's atmosphere, leading to the aggravation of global warming [11].

There are several kinds of aluminosilicate material, which have been experimented with as geopolymer precursors such as metakaolin, albite feldspar, decomposed granite, coal fly ash and iron blast furnace slag [12,13]. Marls are carbonate-bearing clay sediments composed of a mixture of clay minerals, carbonates, quartz and feldspar in different proportions [14]. These mineral associations provide the aluminosilicate source (e.g., clay minerals and feldspar) required for the synthesis of semi-crystalline to amorphous polymeric ring chains as well as the presence of carbonate. Marl has been studied only as an alternative pozzolanic material for the replacement of Portland cement at different percentages of 20–65%. It was found that the compressive strength of mortar with 50% replacement by calcined marl is nearly equal to that of reference with 100% Portland cement [15]. It was also reported as a useful geopolymer precursor when incorporated with limestone and activated only by sodium silicate [16]. The present study will discuss and shed more light on the synthesis of calcined marl-based geopolymer without any additional incorporation of Portland cement and limestone. Also, the calcined samples will be activated by a mixture of sodium hydroxide and sodium silicate solutions.

2. Materials and Methods

2.1. Materials

The aluminosilicate source is represented here by marl deposits located at the eastern sector of the Abu-Tartur phosphate mine, between latitude 25°25′34.5″ N and longitude 30°05′11.3″ E, in the Western Desert of Egypt. Marl deposits occur as a 3 m-thick, brownish yellow and moderately hard bed, which is overlain by 5 m thick intercalations of shale and limestone and underlain by 18 m-thick alternating beds of phosphorite, black shale and glauconite (Figure 1).

Figure 1. Field photo of the studied marl deposits at the eastern sector of Abu-Tartur phosphate mine (**a**) and a representative hand specimen (**b**).

The presence of an alkali environment is necessary to provide the hydroxyl ions, which initiate the polymerization reaction via dissolution of the aluminosilicate source and the release of the active silica and alumina ion species [17]. Sodium hydroxide pellets (pure pharma grade) have been used for preparing hydroxyl ions-bearing solutions of different concentrations 2.5, 5, 8, 10 and 12.5 M. On the other hand, the alkali activation reaction requires sodium silicate solution, which serves as a catalyst and improving agent for the polycondensation process [18]. In the present study, sodium silicate solution was provided by dissolving 40 g sodium meta-silicate powder (ALPHA CHEMIKA, Mumbai, India) into 100 mL solution on heating. The final activation solution was obtained by a mixture of solutions of sodium hydroxide and sodium silicate.

2.2. Experimental Methods

About 100 g marl sample was pulverized to up to −75 μm using agate mortar for performing chemical and mineralogical assays. The chemical composition was studied using an X-ray fluorescence (XRF) spectrometer (PANalytical-Axios, The Netherlands), while the mineral composition was identified using X-ray diffraction (XRD) (monochromatic Cu kα radiation, λ = 1.540562 Å, 40 kV, 25 mA) and Fourier transform–infrared spectroscopy (FT–IR).

The run-of-mine marl sample, about 100 kg in weight, underwent a comminution process. The outlet particle size was set at −2 mm and −500 μm for jaw crusher and hammer mill, respectively. The size reduction was performed in a closed circuit using mesh #35 until the whole sample reached −500 μm in diameter. Afterwards, the ground sample was split by mechanical splitter to yield a representative sample for further processes.

Generally, the calcination process is an endothermic reaction, which leads to chemical and structural decompositions of the calcined material [19]. The main aim of calcination here is to increase the pozzolanicity of marl. As mentioned, marl deposits consist mainly of mixtures of clay minerals and carbonate at different proportions. On calcination between 500 and 800 °C, clay minerals are dehydroxylated to form a reactive pozzolanic metastable state via losing structural water from the octahedral sheet [20]. Also, the carbonate minerals are calcined and decomposed to CaO, which improves the early strength and setting time of geopolymeric cement due to the formation of calcium-silicate-hydrate gel during the alkali activation reaction with aluminosilicate minerals [21]. In the present study, the ground marl was calcined at 550, 650, 750 and 850 °C using a muffle furnace. XRD and FT–IR assays were conducted on the calcined samples and the results were compared to the results of non calcined samples to monitor the compositional changes during calcination.

The geopolymer paste was synthesized by mixing the calcined ground marl thoroughly with a specific volume of the activation solution at different mixing ratios. The paste was molded in steel cubes (50 × 50 × 50 mm) and shaken to avoid space formation within geopolymer molds. Afterwards, geopolymer cubes were demolded and sealed in oven bags resistant to temperature up to 180 °C. To promote the geopolymerization reaction, the sealed cubes were cured in a drying oven at different curing temperatures (40, 50, 60, 70 and 80 °C) and curing times (1, 6, 12, 24 and 48 h). The compressive strength of the cured cubes was measured after varying aging times of 3, 7, 14, 20 and 28 days. The geopolymerization process is simplified in Figure 2 and the mixing proportions are listed in Table 1.

Table 1. Mixing design of the calcined marl-based geopolymer at 70 °C, 48 h, and 7 days.

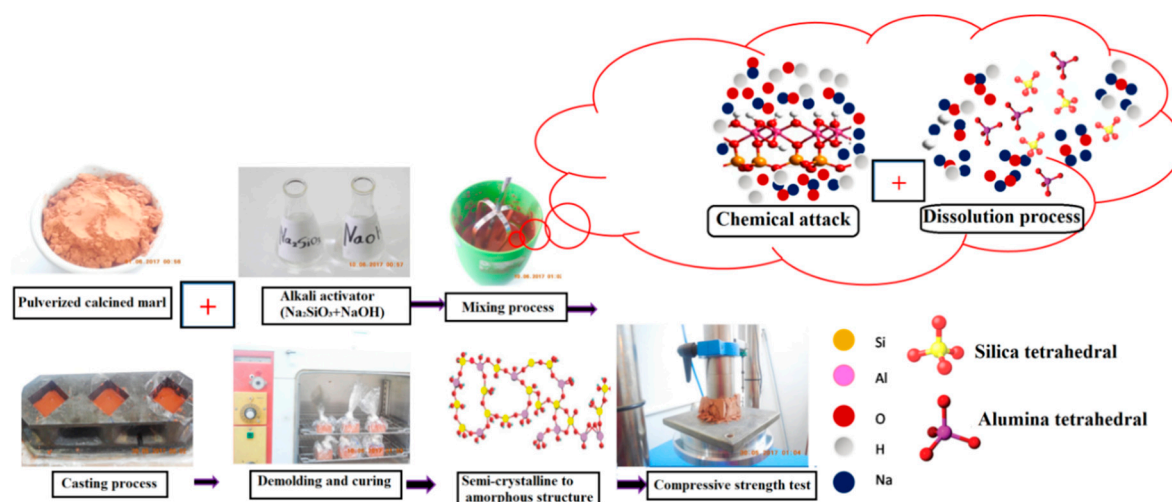| Parameters	Calcined Marl (g)	Sodium hydroxide (SH) (g)	SH (Molarity)	Sodium silicate (SS) (g)	SS/SH Mass Ratios	Solid/liquid (S/L) Mass Ratios	Water (g)
Different NaOH molarities	100	10, 20, 30, 40, and 50	2.5, 5, 8, 10, and 12	40	1.5	2	150, 140, 130, 120, and 110
Different SS/SH mass ratios	100	40	10	40	0.6, 1, 1.5, 2.3, and 3	2	120
Different S/L mass ratios	80, 85, 90, 100, and 110	40	10	40	1.5	1.5, 1.7, 1.8, 2, and 2.2	120

Figure 2. Simplified flowsheet for the synthesis of calcined marl-based geopolymer.

3. Results and Discussion

3.1. Chemical Composition of Aluminosilicate Source

The chemical composition of Abu-Tartur marl sample is listed in Table 2. The studied sample shows a high concentration of SiO_2 reported at 46.95 wt %, which is considered to be an indication of the presence of quartz mineral. Moreover, the Al_2O_3 content 5.88 wt % is much lower than that of CaO 28.0 wt %, indicating the carbonate phase prevailing over the percentage of clay fraction. Regarding alkali oxides, in particular Na_2O and K_2O, they are considered to be critical components in the cement industry due to their reaction with the silica aggregates of concrete, resulting in the formation of alkali-silica gels that cause expansion and disintegration of the building concrete. So, the maximum concentration of these oxides in the aluminosilicate raw materials must be mitigated through the range 0.3–1.2 wt % [22]. The studied marl contains 0.59 wt % of alkalis and hence the resultant geopolymeric cement is not expected to experience future concrete expansion.

Table 2. Major oxides of the studied marl sample (wt %).

SiO_2	Al_2O_3	TiO_2	Fe_2O_3	CaO	MgO	Na_2O	K_2O	MnO	P_2O_5	SO_3	L.O.I	SUM
46.95	5.88	0.60	0.85	28.0	0.73	0.20	0.39	0.13	1.75	0.70	13.73	99.91

3.2. Mineral Composition of Aluminosilicate Source

The interpretation of XRD assays of the non-calcined marl (Figure 3) indicates that both quartz and calcite are the most dominant minerals in the studied sample and this is consistent with what has been previously discussed in the section of chemical composition. The clay fraction is represented by a little amount of saponite. Also, the studied marl is invaded by the sulfate phase, which is dominated by gypsum.

The XRD results have been supported by measuring the infrared (IR) spectra of the marl-forming minerals. As shown in Figure 4, the characteristic absorption bands of calcite appear at 2924, 2853, 2512, 1429, 1087, and 874 cm^{-1} and this is mainly ascribed to the vibration of CO_3 groups contained in the crystal structure of calcite [23]. Quartz is detected at 1087, 798, and 696 cm^{-1}. Saponite is measured at 3627, 3419, and 1087 cm^{-1}. The first two bands are assigned to the absorption of the structural OH groups, while the last is attributed to the vibration of Si-O anions. Gypsum is only detected at the 777 cm^{-1} absorption band.
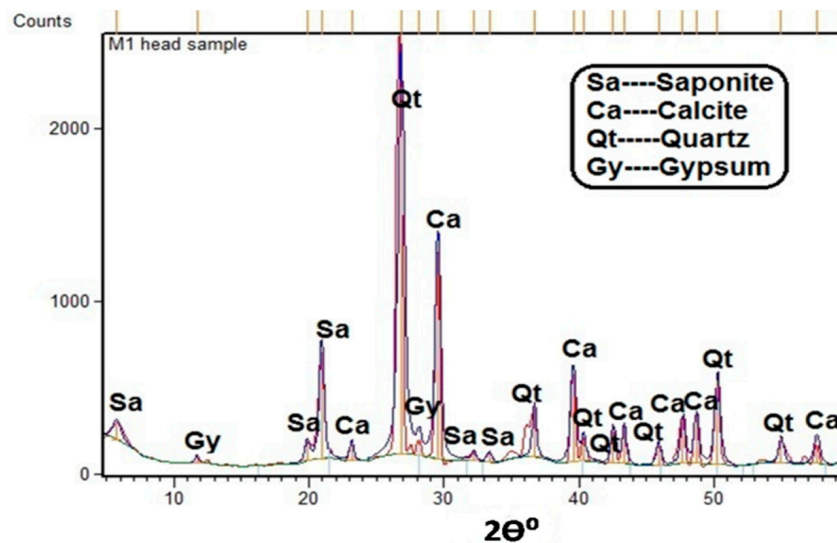
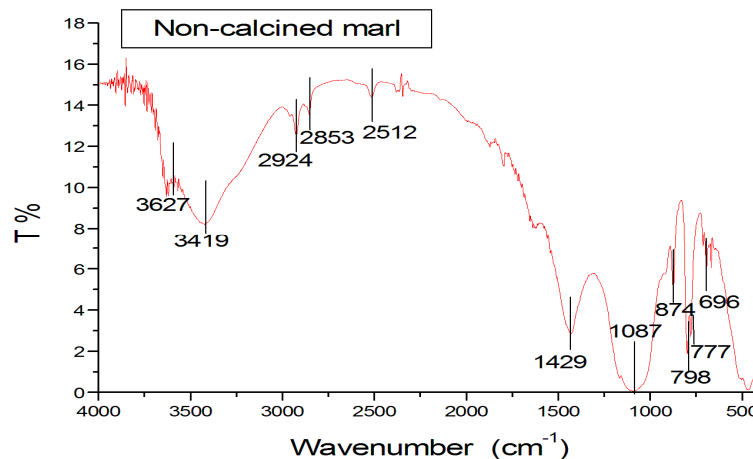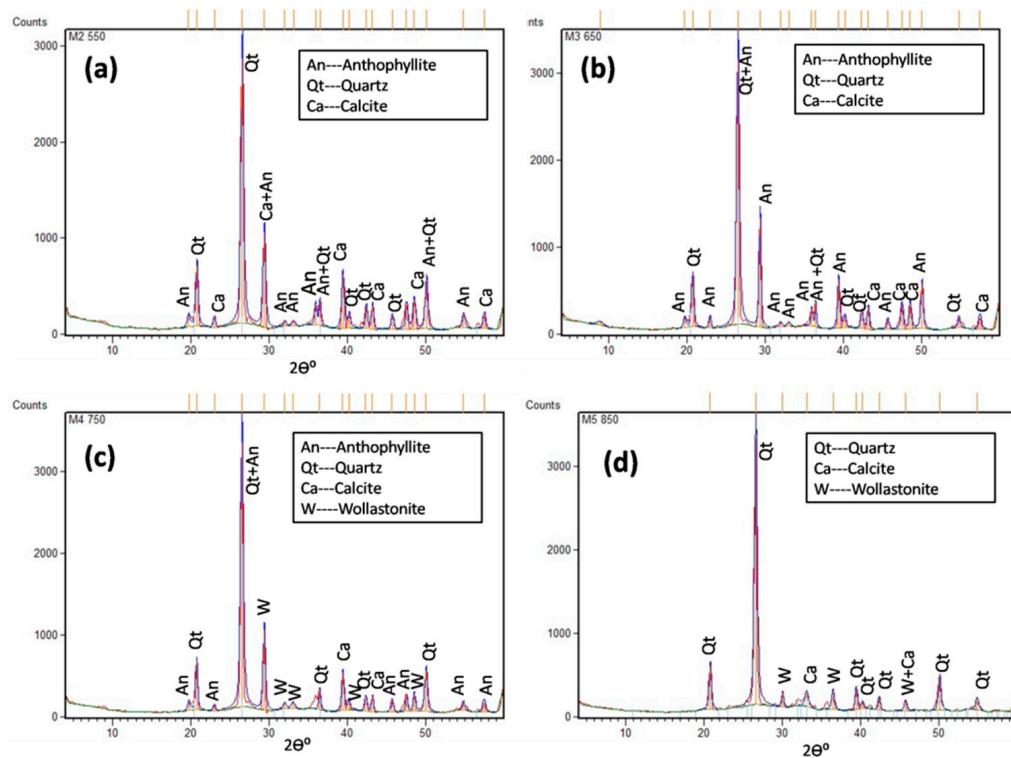**Figure 3.** X-ray diffraction (XRD) pattern of the non-calcined marl sample.

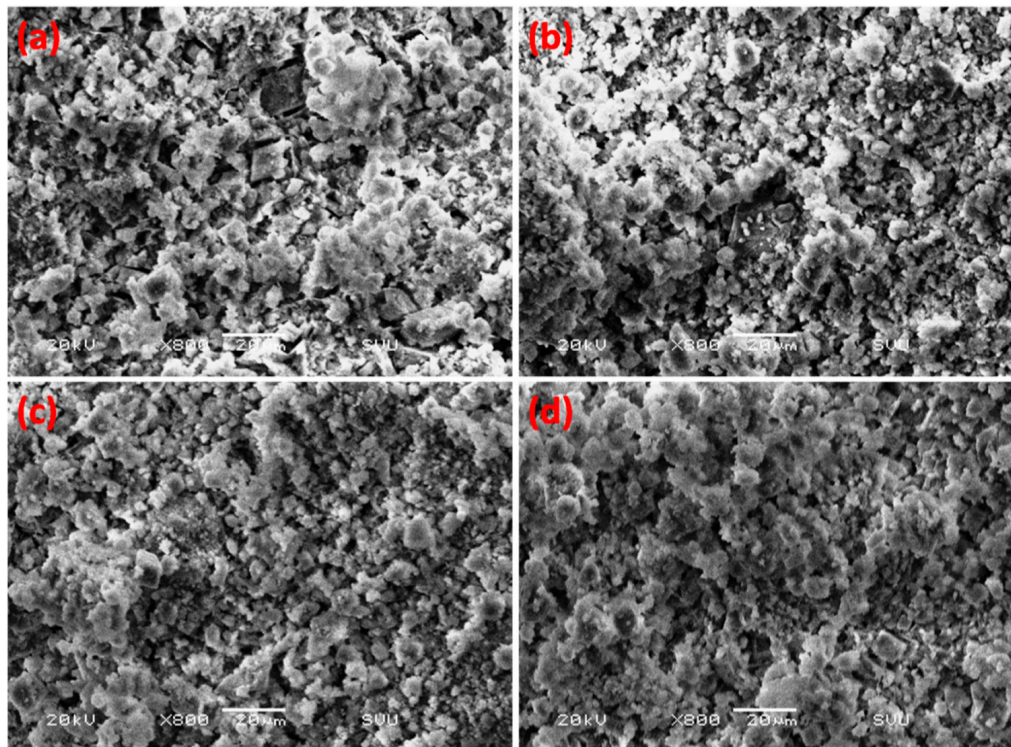**Figure 4.** Fourier transform–infrared spectroscopy (FT–IR) spectra of the non-calcined marl sample.

3.3. Mineral Transformation on Calcination

The mineral transformations of the marl sample were investigated at 550, 650, 750, and 850 °C calcination temperatures using XRD and FT–IR. According to XRD patterns, saponite was completely transformed into anthophyllite and gypsum was degraded at 550 °C (Figure 5a). Anthophyllite along with calcite experienced a progressive decomposition indicated by the gradually decreased number of their peaks through the whole range of calcination (Figure 5a–d). The complete destruction of anthophyllite was reached at 850 °C (Figure 5d). The mineral phase resulted from this destruction is quartz. This is consistent with literature [24] and evidenced by the increased number of quartz peaks at 850 °C. The advanced stage of calcite dissociation was detected at 750 °C by the appearance of wollastonite (Figure 5c), which results from a solid-state reaction between silica and calcium carbonate [25]. The silica content of wollastonite is thought to be derived from the degradation of anthophyllite and the primary quartz of marl sample.

Moreover, the thermal decomposition of calcite has been studied using scanning electron microscopy (SEM). As shown in Figure 6, the calcite grains can still be recognized by their characteristic rhombohedral shape at 550 and 650 °C (Figure 6a,b). However, further heating has led to diffusion of the rhomboherons peripheries as an indication for the advanced stages of calcite crystal lattice destruction (Figure 6c,d).
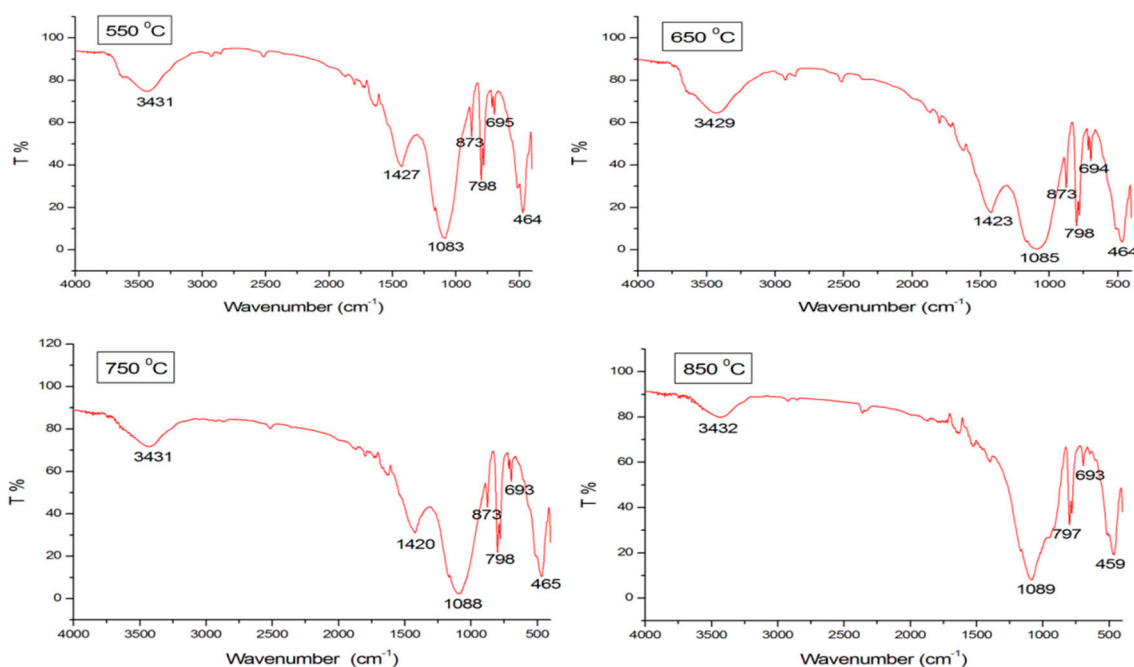
Figure 5. XRD patterns of marl samples at different calcination temperatures (**a**) 550 °C; (**b**) 650 °C; (**c**) 750 °C; and (**d**) 850 °C.

Figure 6. Scanning electron microscope (SEM) micrographs of calcined marl samples showing the diffusion of calcite rhomboherons peripheries on calcination (**a**) 550 °C; (**b**) 650 °C; (**c**) 750 °C; and (**d**) 850 °C.

Regarding FT–IR (Figure 7), the characteristic absorption bands 3627 and 3419 cm^{-1} of saponite disappeared at 550 °C and the vibrational band 464 cm^{-1} of anthophyllite was detected, indicating the complete transformation of saponite into anthophyllite. Under the same calcination conditions, the vibration band 777 cm^{-1} of gypsum was destroyed, whereas calcite was still reported at three absorption bands 3431, 1427, and 873 cm^{-1} due to the vibration of CO_3 group. Also, the detection of 1084, 695, and 798 cm^{-1} caused by Si–O–Si and O–Si–O bonds emphasize the presence of quartz. With increasing the calcination temperature, both calcite and anthophyllite were subjected to thermal dissociation. The gradual decomposition of calcite is inferred by noticeable decrease of its absorption band 1427 cm^{-1} up to 1420 cm^{-1} at 750 °C and then completely disappeared along with the bending band 873 cm^{-1} at 850 °C. Also, the complete destruction of anthophyllite occurred at 850 °C, resulting in the appearance of an additional bending band of quartz at 458 cm^{-1}. The dominant occurrence of silica along with the degraded calcite led to a solid state reaction whose final product was wollastonite, which first appeared at 750 °C and vibration band 1088. The nucleation rate of wollastonite augmented at 850 °C, resulting in additional absorption bands 693 cm^{-1}.
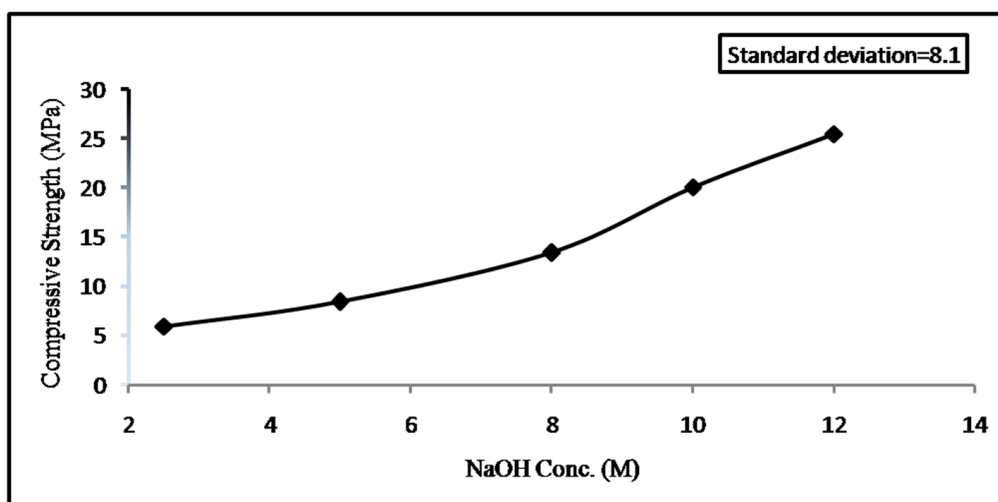

Figure 7. Fourier transform–infrared (FT–IR) spectra of marl samples calcined at different temperatures.

3.4. Compressive Strength Performance
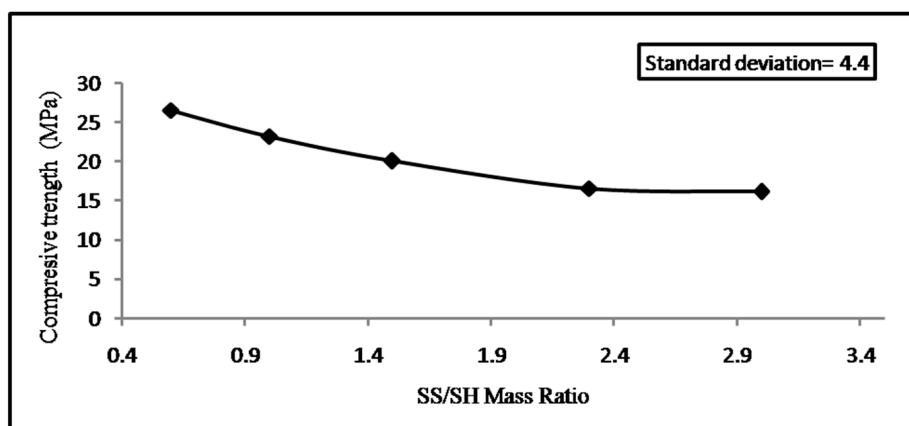
3.4.1. Effect of NaOH Concentration

The present work studied the compressive strength performance of calcined marl-based geopolymer at different NaOH molarities of 2.5, 5, 8, 10 and 12 M. The other parameters were fixed at 1.5 sodium silicate/sodium hydroxide (SS/SH) mass ratio, 2 solid/liquid (S/L) mass ratio, 70 °C, 48 h, and 7 days. It has been found that the compressive strength is proportional to the concentration of NaOH solution and reaches the maximum value 25.48 MPa at 12 M (Figure 8). The literature [26,27] showed that the increase in the concentration of hydroxyl ions leads to the following reaction processes: (1) the liberation of Si and Al ion species from aluminosilicate raw materials; (2) the formation of stronger ion pairs; and (3) the acceleration of polycondensation rates. These processes all contribute to the development of geopolymer strength.

Figure 8. The effect of NaOH molarities on the compressive strength of calcined marl-based geopolymer.

3.4.2. Effect of Na_2SiO_3/NaOH (Sodium Silicate/Sodium Hydroxide (SS/SH)) Mass Ratio
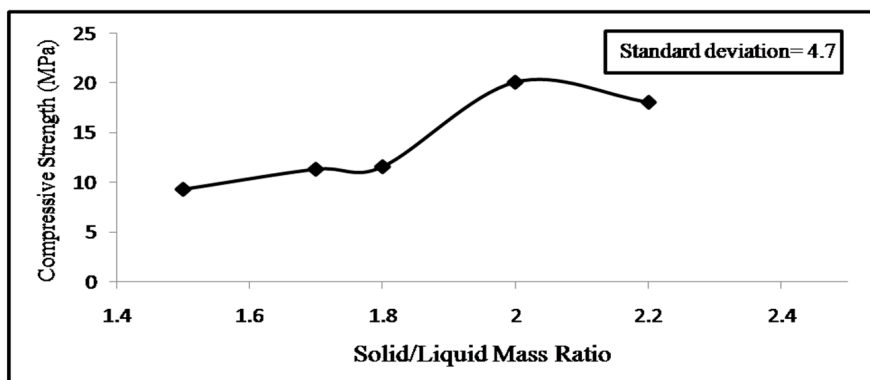
The mixture of sodium silicate (SS) and sodium hydroxide (SH) solutions is considered to be the most common activation solution used for geopolymer synthesis. The mixing proportions strongly affect the rate of geopolymerization reaction and the grade of compressive strength. For instance, during geopolymerization both silica and alumina tetrahedrals are linked to each other by sharing all oxygen atoms. The negative charge of this bonding is balanced by positive ions such as Na^+, K^+ and Ca^{++} [1,5,6]. The mixture of SS and SH is an important supply of Na^+, Si^{+4} and OH^- ion species; therefore, the high ratios of SS/SH will result in the following: (1) balance the negative charge of geopolymer ring chains; (2) high degrees of geopolymerization; (3) high SiO_2/Al_2O_3 ratio which in turn creates more Si–O–Si bonds that are stronger than Si–O–Al bonds; and (4) enhancement of the compressive strength of geopolymer paste [28]. To study this effect, the calcined marl-based geopolymer was built up here at varying SS/SH mass ratios (0.6, 1, 1.5, 2.3 and 3) and under constant conditions of 10 M NaOH, 2 S/L mass ratio, 70 °C, 48 h, and 7 days. The compressive strength was measured and plotted at each mass ratio. The overall results indicate the reverse response of compressive strength to the increase of SS/SH mass ratio as illustrated in Figure 9. For example, the maximum strength value 26.55 MPa is plotted at 0.6 SS/SH mass ratio, while the minimum 16.13 MPa is achieved by increasing the mixing proportion up to 3. The strength behavior here contrasts with the aforementioned literature. This controversy can be ascribed to the gradual decrease of OH^- ion species responsible for the degradation of aluminosilicate lattice and the presence of Ca^{++} ions released from the silicate lattice of calcined marl during the alkali activation reaction. Ca^{++} ions already contribute to balance the negative charge of Si–O–Al bonds. Hence, sodium ions liberated from SS/SH mixtures are in excess, which hinders the polycondensation reaction, may react with the atmospheric CO_2 causing carbonation and retards the development of compressive strength [29]. Moreover, the NaOH molarity used here is fixed at 10 M. The low molarity was compensated at 0.6 SS/SH mass ratio (Figure 9). However, the increased proportion of sodium silicate at the expense of NaOH of low molarity has strongly revealed the deficiency of OH^- ion species. So, the strength failure here can be attributed to the increased Si^{+4} species and the decreased NaOH molarity.

Figure 9. The effect of SS/SH mass ratios on the compressive strength of calcined marl-based geopolymer.

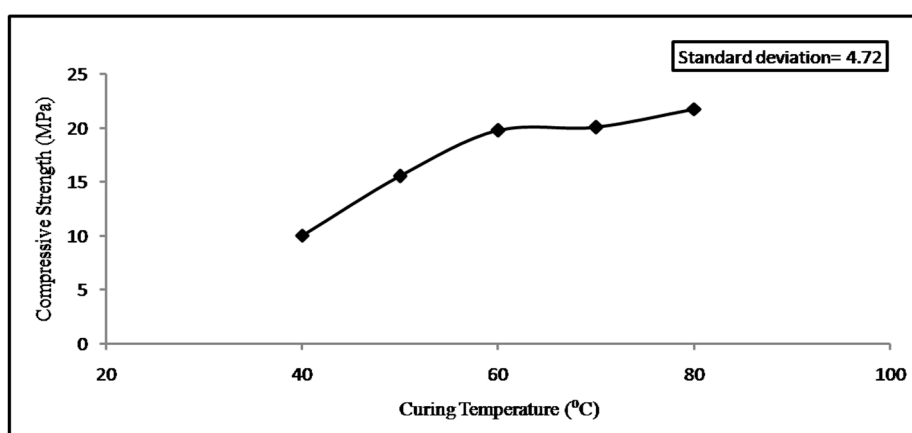### 3.4.3. Effect of Solid/Liquid (S/L) Mass Ratio

The effect of S/L mass ratios on the geopolymer strength was studied at 10 M NaOH, 1.5 SS/SH mass ratio, 70 °C, 48 h, and 7 days. The results have showed that the compressive strength of calcined marl-based geopolymer gradually increases with the increase of S/L mass ratio (Figure 10). The strength peaked at 20 MPa at 2 S/L mass ratio, and then dropped to 18.05 MPa at 2.2 S/L mass ratio. No strength measurement has been conducted at S/L mass ratios higher than 2.2 since the mixture has low workability for good compaction. The performance of compressive strength here is consistent with what has been documented in literature [29,30].The increment of S/L mass ratio means less water for the mixing process, resulting in a faster hardening of the aluminosilicate gel and more rapid linking of the geopolymer ring chains [30]. However, the too-high level of S/L mass ratio seriously influences the compressive strength as reported at 2.2 S/L mass ratio. It creates high sticky slurry due to the increased of non-dissolved aluminosilicate particles, giving a non-homogeneous mixture associated with low compacted paste. On the other hand, the low levels of S/L mass ratio improve the homogeneity and workability of geopolymer slurry. In this case, there is a high content of the activation solution, which may lead to the incorporation of many air bubbles in the geopolymer structure. Hence, the porosity degree is expected to increase that negatively affects the geopolymer strength. Additionally, Na^+ ions will be in excess and react with the atmospheric CO_2 causing carbonation and reduction in the geopolymer strength [29]. However, the porous structure of the geopolymer has found to increase the adsorption capacity of the geopolymer toward heavy metals like cadmium [31].

Figure 10. The effect of S/L mass ratios on the compressive strength of calcined marl-based geopolymer.
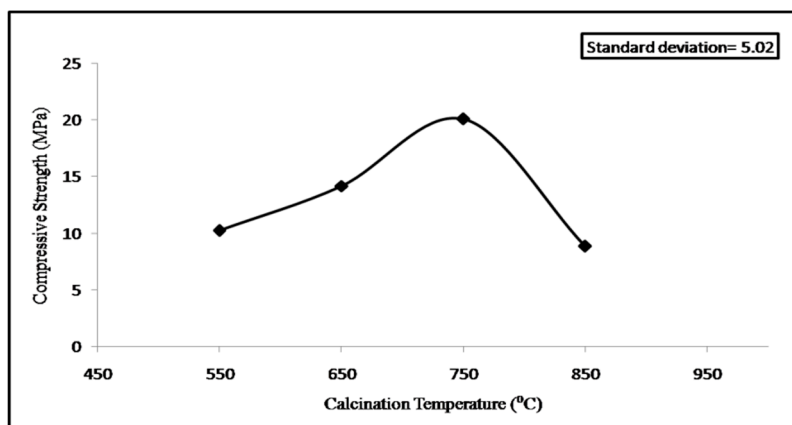
3.4.4. Effect of Curing Temperatures

The alkali activation of the aluminosilicate source takes places through exothermic processes at curing temperatures between 30 and 90 °C. The curing temperature controls the rate of geopolymerization reaction and affects the compressive strength of the geopolymer [1,2]. At this point, the calcined marl-based geopolymer was synthesized at different curing temperatures of 40, 50, 60, 70 and 80 °C under constant conditions of 10 M NaOH, 1.5 SS/SH mass ratio, 2 S/L mass ratio, 48 h, and 7 days. The readings of compressive strength indicate a positive response to the increment of curing temperature. The maximum strength value was measured at 21.76 MPa at 80 °C (Figure 11). The elevation of curing temperature is known to increase the activity of hydroxidyl ions, resulting in high dissolution rates of Si and Al precursors and the acceleration of polycondensation rates and the formation of hard structures. These consequences all enforce the compressive strength of the geopolymer [32].

Figure 11. The effect of curing temperatures on the compressive strength of calcined marl-based geopolymer.

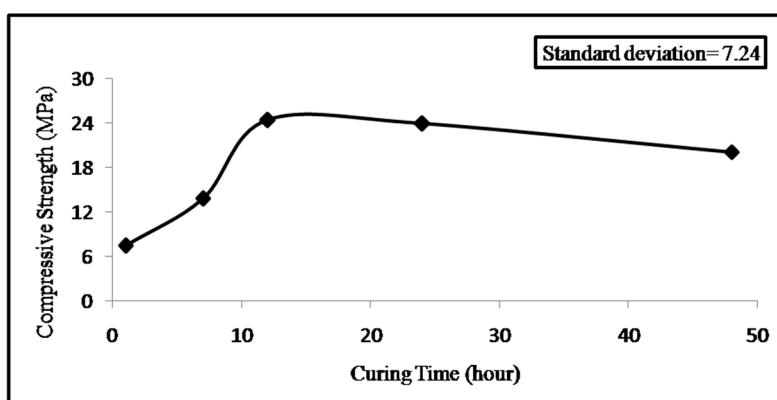### 3.4.5. Effect of Calcination Temperatures

The main aim of calcination is a thermal activation of the aluminosilicate source to increase its pozzolanicity during the alkali activation reaction [33]. The present study has shed light on the strength efficiency of marl-based geopolymer calcined at various temperatures of 550, 650, 750 and 850 °C. The results revealed that the compressive strength increases from 10.23 to 20.08 MPa when elevating temperature from 550 to 750 °C (Figure 12). The increase of strength performance with the increment of calcination is interpreted as a result of the increase of dehydroxylation and decarbonation of aluminosilicate source, which results in an increase in the formation of both more reactive metastable phase and CaO. This strengthening behavior as a function of calcination temperature is also documented in literature [33,34]. Although a faster hardening of geopolymer paste was observed at 850 °C, the strength measurements quickly dropped to 8.86 MPa. The faster hardening is attributed to the high content of CaO formed at 850 °C, which makes the reaction of the aluminosilicate source with alkali solution occur rapidly [21]. However, the too-high calcination temperature (e.g., 850 °C) is not preferable for geopolymer synthesis from clayey aluminosilicate materials. This leads to a decrease in the occurrence of the disordering and metastable phase inside the crystal structure of the aluminosilicate source, resulting in declining pozzolanicity and compressive strength of the resultant geopolymer [33]. This hypothesis is supported by the XRD patterns of calcined samples that show the dominance of the unreactive crystalline phases at 850 °C including wollastonite and quartz.

Figure 12. The effect of calcination temperatures on the compressive strength of calcined marl-based geopolymer.

3.4.6. Effect of Curing Time

Curing time is considered to be among factors that critically affect the compressive strength of geopolymers. The present study investigated the effect of five time intervals (1, 6, 12, 24 and 48 h) on the strength development of calcined marl-based geopolymer at 10 M NaOH, 1.5 SS/SH mass ratio, 2 S/L mass ratio, 70 °C, and 7 days. The results showed that the compressive strength was well developed (24.42 MPa) at 12 h curing time and then declined up to 20 MPa at 48 h further exposure (Figure 13). This is consistent with literature [32], which showed that the increase in curing time allows further dissolution of Si and Al species to occur from the amorphous phase present in the aluminosilicate source. However, prolonged curing time at high curing temperature (e.g., 70 °C in the present study) leads to strength failure due to the concentration of aluminosilicate gel without converting it into a more semi-crystalline phase, resulting in a breakdown of geopolymer structure. Also, the prolonged curing time results in dehydration and excessive shrinkage that weaken the compressive strength.
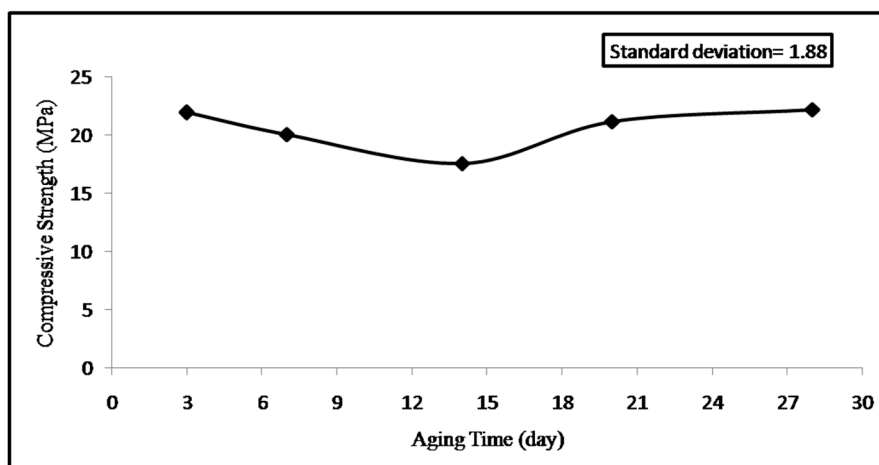

Figure 13. The effect of curing time on the compressive strength of calcined marl-based geopolymer.

3.4.7. Effect of Aging Time

The effect of aging time was investigated at various intervals including 3, 7, 14, 20, 24, and 28 days and constant 10 M NaOH, 1.5 SS/SH mass ratio, 2 S/L mass ratio, 70 °C, and 48 h. The compressive strength of calcined marl-based geopolymer is slightly enhanced by increasing the aging time interval (Figure 14). It already reached 22.21 MPa on day 28. This positive correlation is also documented in literature [6]. The positive relation between aging time and compressive strength is ascribed to the tight seal of geopolymer cubes until the day of the strength test. The importance of the sealing procedure is to

prevent moisture loss from the ambient atmosphere around the geopolymer cubes. It has been proven that the unsealed cured geopolymer samples experience moisture loss and carbonation, resulting in a retardation of the geopolymerization process [35]. This is illustrated by the decreased strength of the unsealed cube at 14 days. In general, water is important for the alkali activation reaction and is consumed during the dissolution of aluminosilicate source. During hydrolysis and condensation processes, water is released into the ambient atmosphere [5]. The water retention after heated curing contributes to improvement in the compressive strength of the geopolymer, which can continue growing for several aging years [36].

Figure 14. The effect of aging time on the compressive strength of calcined marl-based geopolymer.

4. Conclusions

The Abu-Tartur marl deposit has been investigated for its feasibility as a geopolymer precursor after adequate calcination at 550, 650, 750, and 850 °C for one hour. Two scenarios have been produced by the calcination process. The first one is a thermal decomposition of both calcite and saponite, which contributed to the increment of geopolymer strength. The second one is represented by the increased percentage of the unreactive crystalline phases on further heating that led to a gradual decrease of the resultant strength.

There is a proportional relationship between the compressive strength of calcined marl-based geopolymer and NaOH concentration, S/L mass ratio, curing temperature, calcination temperature, and aging time. All of these parameters have played a vital role in the dissolution of the aluminosilicate source and enhancing the rate of the geopolymerization reaction. The optimum strength was developed at 12 M NaOH, 2 S/L mass ratio, 80 °C curing temperature, 750 °C calcination temperature, and 28 days aging time.

One controversial result is that a reverse behavior of the compressive strength has been reported with the increase of SS/SH mass ratio due to the gradual decrease of OH^- ion species responsible for the degradation of the aluminosilicate lattice and the presence of Ca^{++} ions released from the silicate lattice, which crowd out sodium ions liberated from SS/SH mixtures. Moreover, the prolonged curing time above 12 h at 70 °C results in strength failure due to the concentration of aluminosilicate gel without converting it into a more semi-crystalline phase.

Last but not least, the synthesized marl-based geopolymer can be a candidate for construction purposes and water treatment. The former application will require a well-compacted internal structure, while the latter prefers a porous internal structure that can be obtained at low S/L mass ratios.

References

1. Davidovits, J. Geopolymers: Inorganic polymeric new materials. *J. Therm. Anal. Calorim.* **1991**, *35*, 429–441. [CrossRef]
2. Chindaprasirt, P.; Chareerat, T.; Sirivivatnanon, V. Workability and strength of coarse high calcium fly ash geopolymer. *Cem. Concr. Compos.* **2007**, *29*, 224–229. [CrossRef]
3. Mobili, A.; Belli, A.; Giosuè, C.; Bellezze, T.; Tittarelli, F. Metakaolin and fly ash alkali-activated mortars compared with cementitious mortars at the same strength class. *Cem. Concr. Res.* **2016**, *88*, 198–210. [CrossRef]
4. Duxson, P.; Fernández-Jiménez, A.; Provis, J.L.; Lukey, G.C.; Palamo, A.; Van Deventer, J.S.J. Geopolymer technology: The current state of art. *J. Mater. Sci.* **2007**, *42*, 2917–2933. [CrossRef]
5. Rovanik, P. Effect of curing temperature on the development of hard structure of metakaolin-based geopolymer. *Constr. Build. Mater.* **2010**, *27*, 1176–1183. [CrossRef]
6. Favier, A.; Habert, G.; Roussel, N.; de Laceillerie, J.B. A multinuclear static NMR study of geopolymerisation. *Cem. Concr. Res.* **2015**, *75*, 104–109. [CrossRef]
7. Zhang, Y.; Sun, W.; Chen, Q.; Chen, L. Synthesis and heavy metal immobilization behaviors of slag based geopolymer. *J. Hazard. Mater.* **2007**, *143*, 206–213. [CrossRef] [PubMed]
8. Colangelo, F.; Roviello, G.; Ricciotti, L.; Ferrándiz-Mass, V.; Messina, F.; Ferone, C.; Tarallo, O.; Cioffi, R.; Cheeseman, C.R. Mechanical and thermal properties of lightweight geopolymer composites. *Cem. Concr. Compos.* **2018**, *86*, 266–272. [CrossRef]
9. Monteiro, P.J.; Mehta, M.P. *Concrete: Structure, Properties and Materials*, 2nd ed.; Prentice Hall: Upper Saddle River, NJ, USA, 1993; pp. 21–23.
10. Worrell, E.; Price, L.; Martin, N.; Hendriks, C.; Meida, L.O. Carbon dioxide emissions from the global cement industry. *Annu. Rev. Energy Environ.* **2001**, *26*, 303–329. [CrossRef]
11. Mehta, P. Reducing the environmental impact of concrete. *Concr. Int.* **2001**, *23*, 61–66.
12. Dassekpo, J.B.M.; Zha, X.; Zhan, J. Compressive strength performance of geopolymer paste derived from Completely Decomposed Granite (CDG) and partial fly ash replacement. *Constr. Build. Mater.* **2016**, *138*, 195–203. [CrossRef]
13. Temuujin, J.; Williams, R.P.; van Riessen, A. Effect of mechanical activation of fly ash on the properties of geopolymer cured at ambient temperature. *J. Mater. Process. Technol.* **2009**, *209*, 5276–5280. [CrossRef]
14. Bucher, K.; Grapes, R. *Petrogenesis of Metamorphic Rocks*, 8th ed.; Springer: Berlin/Heidelberg, Germany, 2011; pp. 315–316.
15. Danner, T.; Justnes, H.; Norden, G.; Østnor, T. Feasibility of Calcined Marl as an Alternative Pozzolanic Material. In *Calcined Clays for Sustainable Concrete*; Scrivener, K., Favier, A., Eds.; Springer: Dordrecht, The Netherlands; Heidelberg, Germany; New York, NY, USA, 2015; pp. 67–73.
16. Rakhimova, N.R.; Rakhimov, R.Z.; Morozov, V.P.; Gaifullin, A.R.; Potapova, L.I.; Gubaidullina, A.M.; Osin, Y.N. Marl-based geopolymers incorporated with limestone: A feasibility study. *J. Non-Cryst. Solids* **2018**, *492*, 1–10. [CrossRef]
17. Bakharev, T. Durability of geopolymer materials in sodium and magnesium sulfate solutions. *Cem. Concr. Res.* **2005**, *35*, 1233–1246. [CrossRef]
18. Fernández-Jiménez, A.; Gracía-Lodeiro, I.; Palomo, A. Durability of alkali-activated fly ash cementitious materials. *J. Mater. Sci.* **2007**, *42*, 3055–3065. [CrossRef]
19. Mikulčić, H.; von Berg, E.; Vujanović, M.; Priesching, P.; Perković, L.; Tatschl, R.; Duić, N. Numerical modeling of calcination reaction mechanism for cement production. *Chem. Eng. Sci.* **2012**, *69*, 607–615. [CrossRef]
20. Baronio, G.; Binda, L. Study of the pozzolanity of some bricks and clays. *Constr. Build. Mater.* **1997**, *11*, 41–46. [CrossRef]
21. Buchwald, A.; Dombrowski, K.; Weil, M. The influence of calcium content on the performance of geopolymeric binder especially the resistance against acids. In Proceedings of the World Geopolymer, St. Quentin, France, 29 June–1 July 2005; pp. 35–39.

22. Neville, A.M. *Properties of Concrete*, 4th ed.; Wiley: New York, NY, USA; Longmont, CO, USA; London, UK, 2002; pp. 840–844.

23. Andersen, F.; Brečević, L. Infrared Spectra of Amorphous and Crystalline Calcium Carbonate. *Acta Chem. Scand.* **1991**, *45*, 1018–1024. [CrossRef]

24. Mukherjee, S. *Applied Mineralogy: Applications in Industry and Environment*, 1st ed.; Springer Science & Business Media: Dordrecht, The Netherlands, 2011; pp. 65–73.

25. Abd Rashid, R.; Shamsudin, R.; Abdul Hamid, M.A.; Jalar, A. Low temperature production of wollastonite from limestone and silica sand through solid-state reaction. *J. Asian Ceram. Soc.* **2014**, *2*, 77–81. [CrossRef]

26. Xu, H.; Van Deventer, J. The Geopolymerisation of Alumino-silicate Minerals. *Int. J. Miner. Process.* **2000**, *59*, 247–266. [CrossRef]

27. Hardjito, D.; Cheak, C.; Ing, C. Strength and setting times of low calcium fly ash-based geopolymer mortar. *Mod. Appl. Sci.* **2008**, *2*, 3–11. [CrossRef]

28. Al Bakri, A.M.M.; Kamarudin, H.; Omar, A.K.; Norazian, M.N.; Ruzaidi, C.M.; Rafiza, A.R. The Effect of Alkaline Activator Ratio on the Compressive Strength of Fly Ash-Based Geopolymers. *Aust. J. Basic Appl. Sci.* **2011**, *5*, 1916–1922.

29. Liew, Y.; Kamarudin, H.; Al Bakri, A.M.; Luqman, M.; Nizar, I.K.; Ruzaidi, C.M.; Heah, C.Y. Processing and characterization of calcined kaolin cement powder. *Constr. Build. Mater.* **2012**, *30*, 794–802. [CrossRef]

30. Abdul Rahim, R.H.; Azizli, K.A.; Man, Z.; Nuruddin, M.F. Effect of Curing Conditions on the Mechanical Properties of Fly Ash-Based Geopolymer without Sodium Silicate Solution. In Proceedings of the Third International Conference and Exhibition on Sustainable Energy and Advanced Material, Frankfurt am Main, Frankfurt am Main, Germany, 4–6 June 2013; pp. 1–6.

31. Alshaaer, M.; El-Eswed, B.; Yousef, R.I.; Khalili, F.; Rahier, H. Development of functional geopolymers for water purification, and construction purposes. *J. Saudi Chem. Soc.* **2016**, *20*, S85–S92. [CrossRef]

32. Khale, D.; Chaudhary, R. Mechanism of geopolymerisation and factors influencing its development: A review. *J. Mater. Sci.* **2007**, *24*, 729–746. [CrossRef]

33. Elimbi, A.; Tchakoute, H.K.; Njopwouo, D. Effects of calcination temperature of kaolinite clays on the properties of geopolymer cements. *Constr. Build. Mater.* **2011**, *25*, 2805–2812. [CrossRef]

34. Geman, R.; Tjondro, R.T.; Anggono, J.; Hardjito, D. Effects of Calcination Temperature of LUSI Mud on the Compressive Strength of Geopolymer Mortar. *Adv. Mater. Res.* **2013**, *626*, 224–228.

35. Criado, M.; Fernández-Jiménez, A.; Palomo, A. Alkali activation of fly ash. Part III: Effect of curing conditions on reaction and its graphical description. *Fuel* **2010**, *89*, 3185–3192. [CrossRef]

36. Škvára, F.; Kopecký, L.; Šmilauer, V.; Bittnar, Z. Material and structural characterization of alkali activated low-calcium brown coal fly ash. *J. Hazard. Mater.* **2009**, *168*, 711–720. [CrossRef] [PubMed]